Published online 21 February 2017

Nucleic Acids Research, 2017, Vol. 45, No. 8 ***4577–4589***
doi: 10.1093/nar/gkx123

Repair of UV-induced DNA lesions in natural *Saccharomyces cerevisiae* telomeres is moderated by Sir2 and Sir3, and inhibited by yKu–Sir4 interaction

Laetitia Guintini[1], Maxime Tremblay[1], Martin Toussaint[1], Annie D'Amours[1], Ralf E. Wellinger[2], Raymund J. Wellinger[1,*] and Antonio Conconi[1,*]

[1]Department of Microbiology and Infectious Diseases, Université de Sherbrooke, 3201 rue Jean-Mignault, Sherbrooke J1E 4K8, Canada and [2]Centro Andaluz de Biología Molecular y Medicina Regenerativa (CABIMER), Universidad de Sevilla, CSIC, Avda Américo Vespucio s/n, Sevilla 41092, Spain

Received April 11, 2016; Revised February 02, 2017; Editorial Decision February 09, 2017; Accepted February 10, 2017

ABSTRACT

Ultraviolet light (UV) causes DNA damage that is removed by nucleotide excision repair (NER). UV-induced DNA lesions must be recognized and repaired in nucleosomal DNA, higher order structures of chromatin and within different nuclear subcompartments. Telomeric DNA is made of short tandem repeats located at the ends of chromosomes and their maintenance is critical to prevent genome instability. In *Saccharomyces cerevisiae* the chromatin structure of natural telomeres is distinctive and contingent to telomeric DNA sequences. Namely, nucleosomes and Sir proteins form the heterochromatin like structure of X-type telomeres, whereas a more open conformation is present at Y'-type telomeres. It is proposed that there are no nucleosomes on the most distal telomeric repeat DNA, which is bound by a complex of proteins and folded into higher order structure. How these structures affect NER is poorly understood. Our data indicate that the X-type, but not the Y'-type, sub-telomeric chromatin modulates NER, a consequence of Sir protein-dependent nucleosome stability. The telomere terminal complex also prevents NER, however, this effect is largely dependent on the yKu–Sir4 interaction, but Sir2 and Sir3 independent.

INTRODUCTION

Chromatin affects transcription, replication and DNA repair efficiency (1–4). In *Saccharomyces cerevisiae*, throughout the text referred to as yeast, transcription is repressed in condensed heterochromatin-like structures, for example the inactive copies of the *MAT* locus that are sheltered in silent mating type loci (*HML* and *HMR*). At these loci, heterochromatin forms through the nucleation of Sir proteins at silencer elements (E and I), followed by the spreading of the Sir complex. The silent-information regulator genes (*SIR1*, *2*, *3* and *4*) are non-essential for cell growth but are required for transcriptional repression. Initial analyses by chromatin immunoprecipitation (ChIP) suggested that Sir2, Sir3 and Sir4 proteins were present throughout the silenced *HM* loci (5,6). More recently, ChIP followed by next-generation sequencing (ChIP-seq) indicated that Sir proteins were mostly present at silencers and closely adjacent regions, with some enrichment over the *HML* and *HMR* promoters (7). Additionally, precisely positioned nucleosomes were mapped on regions flanking the silencers, and in strains lacking Sir3 nucleosome positioning was lost over half of the silent *HML* locus (8,9).

Telomeres are formed by chromosome terminal-telomeric repeat DNA and telomere associated X and Y' DNA elements (Supplementary Figure S1), and they are thought to be in a heterochromatin-like structure (10). Hence, it was suggested that telomere proximal-gene silencing was caused by telomeric heterochromatin. However, this was reported for synthetic telomeres with the *URA3* reporter gene inserted at various distances from the telomeric DNA (11). The results suggested that silencing of *URA3* decreased with increasing distance from the telomere, which led to the conclusion that yeast telomeres could repress transcription of nearby genes, a phenomenon termed telomere position effect (TPE) (11,12). TPE required outward spreading of Sir2, Sir3 and Sir4 containing chromatin (13,14), together with the heterodimeric yKu complex (15,16). Of note, the telomeres analyzed in those studies did not have the natural sub-telomeric X or Y' elements. In opposition to the silencing spreading-model, investigations on natural telomeres indicated that Sir

*To whom correspondence should be addressed. Tel: +1 819 821 8000 (Ext. 75360); Fax: +1 819 820 6831; Email: Antonio.Conconi@usherbrooke.ca
Correspondence may also be addressed to Raymund J. Wellinger. Tel: +1 819 821 8000 (Ext. 75214); Fax: +1 819 820 6831; Email: Raymund.Wellinger@usherbrooke.ca

proteins were rather non-homogeneously distributed (17–19). ChIP-seq analyses at high-resolution examined the presence of Sir proteins at telomeres in the absence of reporter genes, either with only the X element or with both X and Y' elements. All three Sir proteins were found on telomeric repeats and in the X element, but not in the Y' element (7,20). Thus, at natural telomeres the Sir proteins occur at discrete sites, rather than in a continuous gradient as postulated from the studies on synthetic telomeres. Moreover, reporter genes engineered within the Y' element, which is mostly located between telomeric repeat sequences (TR) and X elements (Supplementary Figure S1A), were not silenced (21).

The distribution of nucleosomes on telomeres was also investigated. Semi-purified chromosome terminal complexes were found to be nucleosome free, whereas positioned nucleosomes were found in adjacent regions (22). Sequencing DNA from immuno-purified nucleosomes confirmed that telomeric repeats were depleted of nucleosomes and that Y' elements had well positioned nucleosomes. For the X elements, one study described positioned nucleosomes immediately upstream and inside the elements (23), whereas a parallel investigation indicated that the X elements were mostly free of nucleosomes (20). Finally, in addition to Sir proteins and modified histones, gene silencing may be enforced by telomere-clustering and perinuclear localization (24–26). Telomere-clustering is promoted, at least in part, by the heterodimeric yKu protein that directly binds to telomeres (27). In cells lacking yKu, the perinuclear localization of both telomeric DNA and Sir proteins is lost, and TPE is abrogated (15,27,28). Since deletion of *SIR3* or *SIR4* did not change the localization of telomeric DNA, it is proposed that yKu helps tether telomeric DNA to the nuclear envelope (29).

Efficient repair of DNA damage induced by intra- and extra-cellular agents is necessary for the maintenance of genome stability. Nucleotide excision repair (NER) removes UV-induced pyrimidine dimers (PDs), like cyclobutane pyrimidine dimers (CPDs) and 6-4 photoproducts (6,4PDs). They are eliminated in five steps: lesion recognition, DNA unwinding and incision of the DNA strand on both sides of the lesion, excision of a DNA fragment of ∼30 nucleotides, filling of the gap by DNA synthesis, and DNA ligation (30). NER is divided in global genome repair (GG-NER) that removes lesions from inactive DNA, and transcription-coupled repair (TC-NER) that removes lesions only from the transcribed strand (TS) of active genes (30,31). In yeast, GG-NER depends in part on *RAD7/16* (32,33) and TC-NER on *RAD26* and *RAD34* for RNA polymerase II and RNA polymerase I, respectively (33–35). Repair of CPDs by TC-NER is faster than by GG-NER (36,37). In addition, it is well established that nucleosomes modulate the efficiency of NER; repair of linker DNA is generally fast and repair of DNA in the nucleosome center is slow (38–41). Conversely, little is known about NER in heterochromatin (42). In synthetic telomeres, removal of UV-induced DNA lesions was followed in the *URA3* gene inserted at ∼2 kb from the telomere ends. Efficient repair was measured in the active *URA3* of *sir3Δ* cells, whereas partial gene silencing slightly reduced and complete silencing drastically inhibited NER (43). Another report analyzed NER in the *URA3* gene that was inserted at ∼1.75 kb from the telomere of chromosome XIL and of chromosome IIIR, where the reporter gene was inactive and active, respectively. As expected, in *sir2Δ* cells the *URA3* gene on chromosome XIL was activated and, thus, repaired more efficiently. However, *URA3* on chromosome IIIR was already active, yet in *sir2Δ* cells NER was faster than in *SIR2* cells (44). Both studies were based on TPE and synthetic telomeres lacking the sub-telomeric X and, or, Y' elements. Therefore, information on NER in chromatin of natural telomeres remains scarce. Here, NER in heterochromatin was followed in the constitutively silenced *HM* loci, in the X and Y' elements of natural sub-telomeres and in telomeric repeats, in presence or absence of Sir and yKu proteins. The results indicate that in sub-telomeric heterochromatin NER is modulated by Sir proteins stabilized-nucleosomes, and that in telomeric chromatin NER is inhibited by the yKu–Sir4 interaction.

MATERIALS AND METHODS

Yeast strains

Information on BY4741 and related gene deleted strains is available in the *Saccharomyces Genome Deletion Project* web site [http://www-sequence.stanford.edu/group/yeast_deletion_project/deletions3.html] (45) (see also Supplementary Table S1).

Media, growth conditions and UV irradiation

Yeast cells were grown exponentially (∼10^7 cells/ml) in yeast extract-peptone-dextrose (YEPD) at 30°C in a culture tube rotator. After centrifugation, cells were re-suspended in ice cold phosphate buffered saline (PBS) (137 mM NaCl, 2.5 mM KCl, 2 mM KH_2PO_4, 10 mM Na_2HPO_4, pH 7.0) to a final concentration of 2 × 10^7 cells/ml. Cell suspensions were poured into trays to a depth of ∼1 mm and irradiated with a UV dose of 180 J/m^2 (254 nm) measured with a UVX radiometer (Ultra-Violet Products, Upland, CA, USA). Cells were harvested, re-suspended in pre-warmed YEPD and incubated in the dark at 30°C with continuous shaking for different repair times, as indicated.

DNA extraction

As previously described (46), for each repair time point, ∼2 × 10^9 cells were collected, washed with ice cold PBS, suspended in 1.5 ml of nuclei isolation buffer (NIB: 50 mM MOPS, pH 8.0, 150 mM potassium acetate, 2 mM MgCl2, 17% glycerol, 0.5 μM spermine and 0.15 μM spermidine) and transferred to 15 ml polypropylene tubes containing 1.5 ml of glass beads (425–600 μm, Sigma). Yeast were disrupted by vortexing (16 × 30 s pulses with 30 s pauses on ice), the nuclear suspensions collected and the glass beads rinsed two times with 1 ml of NIB. The suspensions were combined, centrifuged for 5 min at 13 krpm and the pellets were re-suspended in 500 μl TE. After addition of 225 μl 3M sodium acetate and 35 μl 10% sodium dodecyl sulphate, the nucleic acids were extracted twice with phenol:chloroform (1:1) and once with chloroform, before precipitation at −20°C in isopropanol. After centrifugation, pellets were re-suspended in 200 μl TE and treated with

RNaseA (10 mg/ml) for 30 min at 37°C, and extracted with phenol:chloroform and chloroform before precipitation at −80°C in ethanol for 20 min. After centrifugation, DNA pellets were rinsed in 70% ethanol, dried and re-suspended in 200 μl TE.

T4 endonuclease V, alkaline gel electrophoresis and Southern blotting

The DNA samples were treated with T4 endonuclease V (T4-V; Epicentre) according to manufacturer's recommendations. After T4-V digestion, ∼1 μg of each DNA sample were separated on 1% alkaline agarose gels. DNA was transferred to Hybond N+ membranes (GE-Healthcare) in 0.4 N NaOH, the radioactive probes were generated using ^{32}P-endlabeled oligo-DNA (Supplementary Table S2); hybridization and washing were done at 30°C as previously described (47).

Primer extension

Labeling of DNA oligonucleotides and primer extensions were done as described in (48), except that 1 μg of DNA, 2 pmol of radiolabeled oligonucleotides and 10 pmol of dNTPs were employed. The samples were denatured at 95°C for 10 min and then chilled on ice before the reaction was started by the addition of 0.2 U of Taq polymerase. The thermocycling program was as following: 95°C for 5 min; 30 cycles of denaturation (95°C for 45 s), annealing (55°C for 5 min) and extension (72°C for 5 min); one final extension at 72°C for 10 min. Then, the samples were precipitated with the addition of 1/10th volume of 3 M sodium acetate, 1 ng of salmon sperm and 2.5× volume of ethanol. After incubation at −20°C for 1 h and centrifugation, the DNA pellets were rinsed in 70% ethanol, dried and re-suspended in sequencing gel-loading buffer (48).

Quantification of CPD yield

Phosphorimages of gels were quantified using ImageQuant software (GE-Healthcare). For the T4-V assay, measurement of CPDs was done as in (49,48). For the primer extension assay, end-labeled DNA products were resolved on DNA sequencing gels (6% acrylamide, 0.35 M urea). The intensity of bands reflects Taq arrests at UV photoproducts and, thus, strong band signals correspond to hot spots for UV lesion formations. Signals were analyzed using ImageQuant by drawing a line tightly around the bands. The density of each band was transferred to an Excel spreadsheet and the frequency (F) of a single photoproduct (or cluster of photoproducts) was measured by quantifying its signal intensity and then divided by the signal of the whole lane. The ratio of signal densities that were measured in the −UV lane was subtracted to correct for signal noise (background). The percent of repair for each photoproduct was plotted over the incubation time, whereby the values measured for 0 h repair corresponded to 100% damage (or 0% repair), and percent of repair = 100 × [F(time 0) − F(repair time point)/F(time 0)].

RESULTS

Sir2, Sir3 and Sir4 delay repair of UV induced DNA lesions in *HM* loci

The yeast mating type is determined by the allele (*MATa* or *MATα*) that is present in the transcriptionally active *MAT* locus, whereas silent copies of the genes are stored at the *HMR* and *HML* loci. To characterize NER in silenced chromatin, we first investigated if Sir2, Sir3 and Sir4 moderated NER in both *HM* loci. Yeast grown to early log phase were UV irradiated and incubated for various lengths of time to allow repair of photoproducts. DNA was isolated from non-irradiated and irradiated wild type (WT), *sir2Δ*, *sir3Δ* and *sir4Δ* cells and then prepared for the T4-V assay, an enzyme that nicks DNA at CPD sites. The DNA probe and restriction enzymes were selected to allow concurrent measurements of repair in *HML*, *HMR* and *MATa* (Figure 1A). After treatment with T4-V, changes in signal intensities of bands (Figure 1B–E, left panels; compare − with + lanes) reflect the number of CPDs that are present in the DNA fragments. For the WT, the results indicated that active *MATa* was repaired faster than both silenced *HM* (Figure 1B). On the contrary, in absence of Sir2, Sir3 or Sir4, CPDs were removed at similar rates from all three loci (Figure 1C–E), indicating that repair of CPDs was less efficient in the presence of Sir proteins. However, Sir proteins occlude the transcription machinery from its cognate DNA sequences (50–52). Consequently, in *sirΔ* strains putative transcription activation of *HM* loci (53,54) could be responsible for enhanced repair by TC-NER (55,56) (Figure 1C–E). To examine this possibility, repair of PDs (CPDs and 6,4PDs) in the *HMR* locus was followed in the non-TS (NTS) and within a 350 bp region downstream of the *a1* gene. This region comprises the I-element and is covered by Sir proteins (Figure 2A). A primer extension technique based on efficient and precise blockage of Taq polymerase by PDs (57) was employed to follow repair in WT and *sir3Δ* cells, at nucleotide resolution (Figure 2B). The top band of the gel (+1792) represents full length-extension of undamaged DNA fragment. The bands below indicate the presence of PDs and their intensity is proportional to the frequency at which they form in the sequence (compare DNA of cells that were either not irradiated; lane U, or irradiated; lane 0 h). Decrease in band intensity (lanes 1, 2 and 4 h) indicates the efficiency at which the corresponding PD is repaired. The quantification of single band signals is presented in Supplementary Figure S2, and the average repair for all PDs in WT and *sir3Δ* cells is shown in Figure 2C. Both datasets confirmed that in a non-transcribed region where PDs were removed by GG-NER, the presence of Sir3 tempered the activity of NER. In addition, Supplementary Figure S2B shows that PDs proximal to each other are repaired with distinct kinetics. This can be explained by the limiting-step in NER, the recognition of DNA damage, which largely depends on the degree of helical distortion produced by the lesion. In chromatin, DNA distortion is modulated at different degrees by the presence of proteins. Thus, depending on the position of PDs on kinked DNA around the protein, their recognition can occur at different

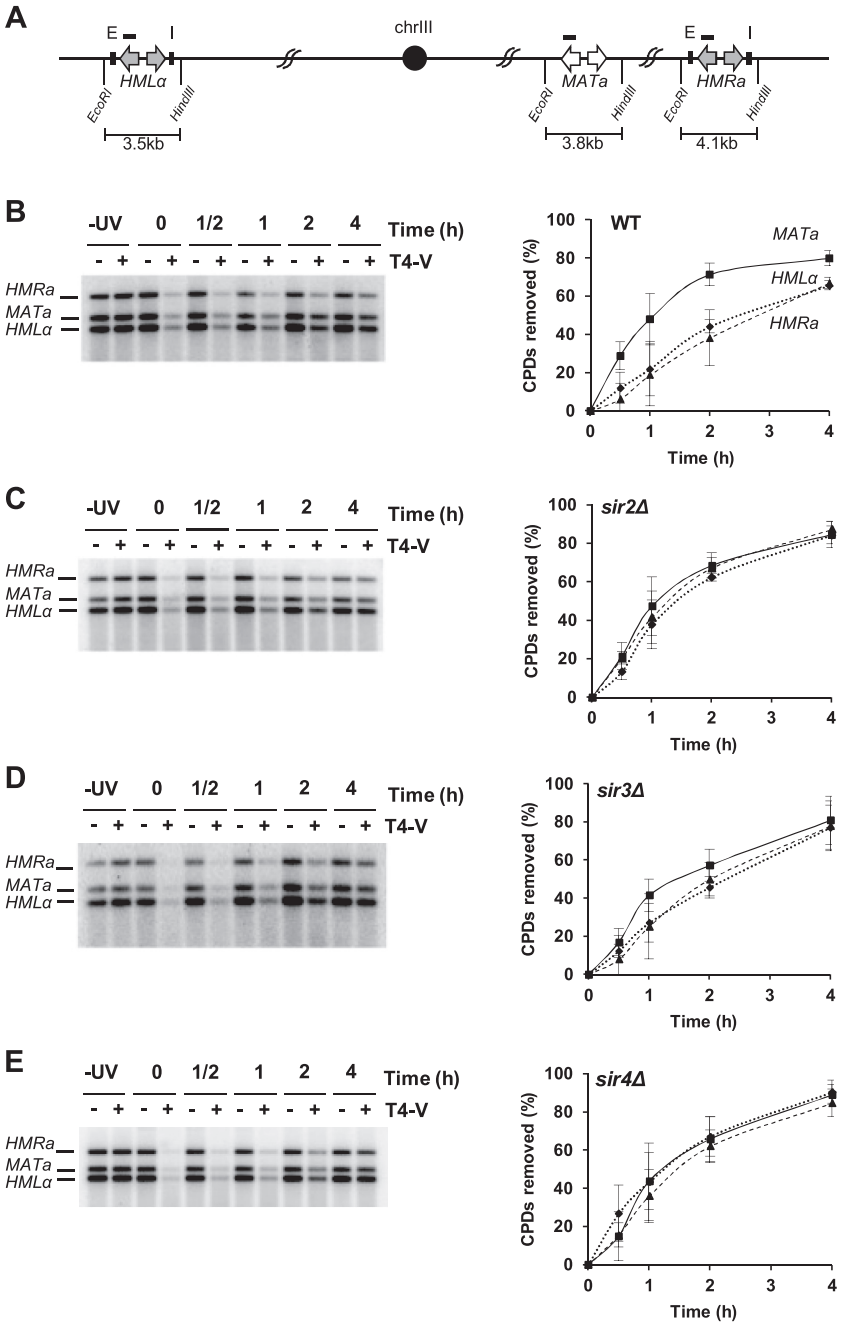

Figure 1. NER in silent *HML*, *HMR* loci and active *MATa* locus. (**A**) Map of the mating type locus on chromosome III. The direction of ORFs (arrows) is indicated, together with the silencer elements (E and I) and restriction sites (EcoRI and HindIII). The restriction fragment lengths are in kilo base pairs and short black bars represent ∼1 kb long double strand DNA probe (size scale is not respected). (**B**–**E**) Yeast WT, *sir2Δ*, *sir3Δ* and *sir4Δ* strains were irradiated at 180 J/m^2 and harvested at the indicated times. Isolated DNA samples from non-irradiated (−UV) and irradiated cells (0–4 h repair) were digested with EcoRI and HindIII. The separation of DNA fragments by denaturing agarose gel electrophoresis and Southern blotting were done as described in 'Materials and Methods' section. Left panels: representative of T4-V assays. Right panels: quantifications of phosphor images with the means ± 1SD of three independent experiments.

rate. This has been shown for gene promoters and nucleosomal DNA (41,58,59).

Sir3 moderates repair of UV induced DNA lesions in the X element chromatin

In contrast to stable silencing at *HM* loci, silencing in subtelomeric regions is variegated and causes stochastic patterns of transcriptional repression (21,60). Given the significant decrease in NER efficiency at silenced *HM* chromatin (Figures 1 and 2), we investigated to what extent heterochromatin at natural telomeres moderated repair. Yeast telomeres are of two classes, one containing a X element abutting the terminal telomeric repeats (X-telomeres) and the other harboring up to four Y' elements between the X ele-

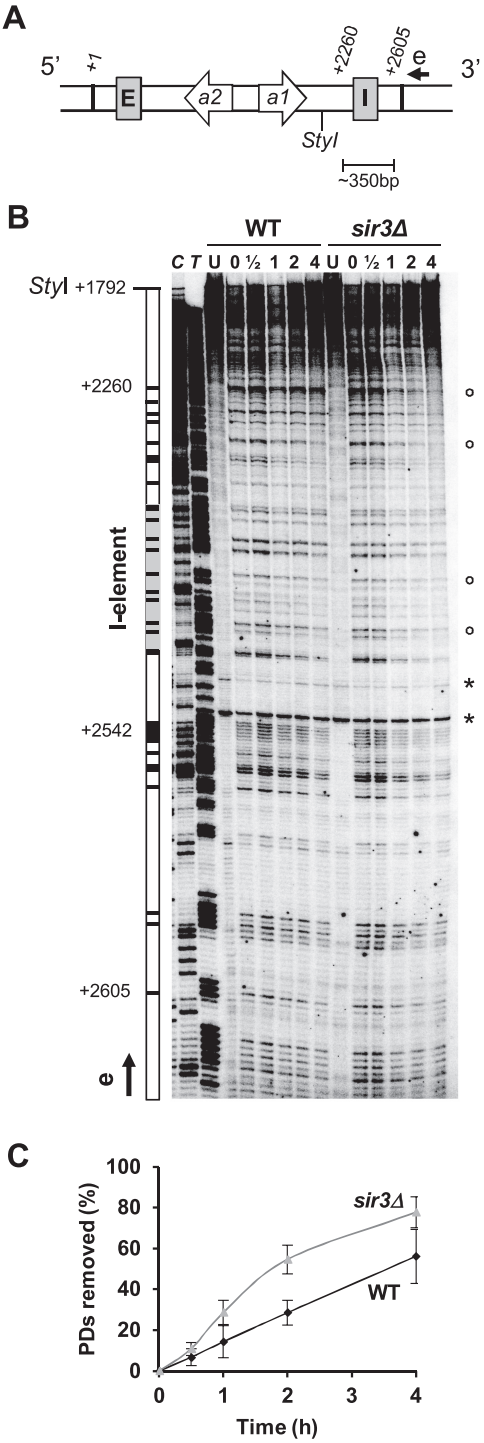

Figure 2. NER in the *HMR* locus, I-element and surrounding region, at nucleotide resolution. (**A**) Map of the *HMR* locus. The position of *a2*- and *a1*- ORFs and direction of transcription are shown, together with the *StyI* restriction site and the fragment length in base pairs. The arrow 'e' indicates the primer and direction of Taq polymerase elongation. The nucleotide sequence starts at position +1, marking the beginning of the *HMR* locus. (**B**) Yeast were grown and prepared as described in Figure 1. The representative sequencing gel illustrates repair of PDs in the upper, non-transcribed strand of WT and *sir3Δ* strains, within ~ 350 bp fragment. Lanes are: C and T, sequencing; U, DNA extracted from non-irradiated cells; 0–4, DNA extracted from cells immediately after irradiation or after 0.5, 1, 2 and 4 h repair. Map on the left side represents portion of the *HMR* locus with the I-element (gray), and the PDs that were quantified (lines for single PDs; boxes for clusters of PDs) with their positions numbered from nucleotide +1. Example of PDs that are repaired faster in *sir3Δ* cells than in WT are shown by circles, stars point to natural Taq-road blocks in the sequence and when PDs formed at these sites they were not quantified. (**C**) Signals were analyzed using ImageQuant by drawing a tight line along the gel lanes. The signal that was measured in the −UV lane was subtracted from the other lanes to correct for background. DNA damage (lane 0) and repair (lanes 0.5 to 4 h) were measured by averaging all PDs in a lane. The percent of repair was plotted over the incubation time, whereby the values obtained for 0 h repair corresponded to 100% damage (or 0% repair). Black line for WT and gray line for *sir3Δ* cells. The data represent means ± 1SD deviation of three independent experiments.

ment and the terminal repeats (Y'-telomeres) (Supplementary Figure S1). It was reported that Sir proteins are enriched on the X elements and on telomeric repeats, but not on Y' elements (7,20). Therefore, to determine the efficiency of NER in heterochromatin at native chromosome ends, repair of UV-induced DNA lesions was measured within the X elements and in flanking sequences (~150 bp). The primer extension technique was employed to compare repair in WT and *sir3Δ* cells at nucleotide resolution (Figure 3), and the quantifications were done as described for the *HMRa* locus (Supplementary Figure S2).

In WT cells and for the strand running 3′ to 5′ toward the telomeres (lower strand) (Figure 3A and B, left panels), PDs throughout the sequence were repaired at different rates. After 4 h, lesions at the telomere distal end of the X element (PDs −16 to −1) were ~49% repaired, whereas lesions in the X element (PDs +1 to +24) were ~38% repaired (Supplementary Figure S3A). For the opposite strand (Figure 3C and D, left panels), after 4 h lesions in the XC region (PDs −3 to +16) were ~50% repaired and in the XR region (PDs +17 to +22) ~41% repaired (Supplementary Figure S3A). When *SIR3* was deleted (right panels), overall removal of PDs was considerably faster with an average repair of ~87% (PDs −16 to −1) and ~ 66% (PDs +1 to +24) for the lower strand, and ~ 78% (PDs −3 to +16) and ~66% (PDs +17 to +22) for the upper strand (Supplementary Figure S3A). Thus, although the Sir complex did not affect the formation of PDs (Figure 3, 0 lanes; compare WT and *sir3Δ*) it considerably decreased NER efficiency throughout the X element. Recent genome wide-mappings of Sir proteins suggest that Sir3 is less prominent at the distal end of the X element (7). If correct, our data suggest that even the lowered level of Sir3 at the distal ends of the X-elements can affect NER efficiency (Supplementary Figure S3B).

Nucleosome distribution and modulation of NER efficiency in the X element

Genome-wide mappings of histones H3 and H4 designated three positioned, canonically spaced nucleosomes at the telomere distal end of the X element (not shown in Figure 4), followed by one strongly positioned nucleosome at the beginning of the X element (nucleosome I), a gap of 330 bp and regularly spaced nucleosomes toward the telomere (nucleosomes II, III, IV) (Figure 4) (23). Yet the occurrence of nucleosomes in the X element is debated (20,23). As stated above, repair efficiency can be modulated by nucleosomes

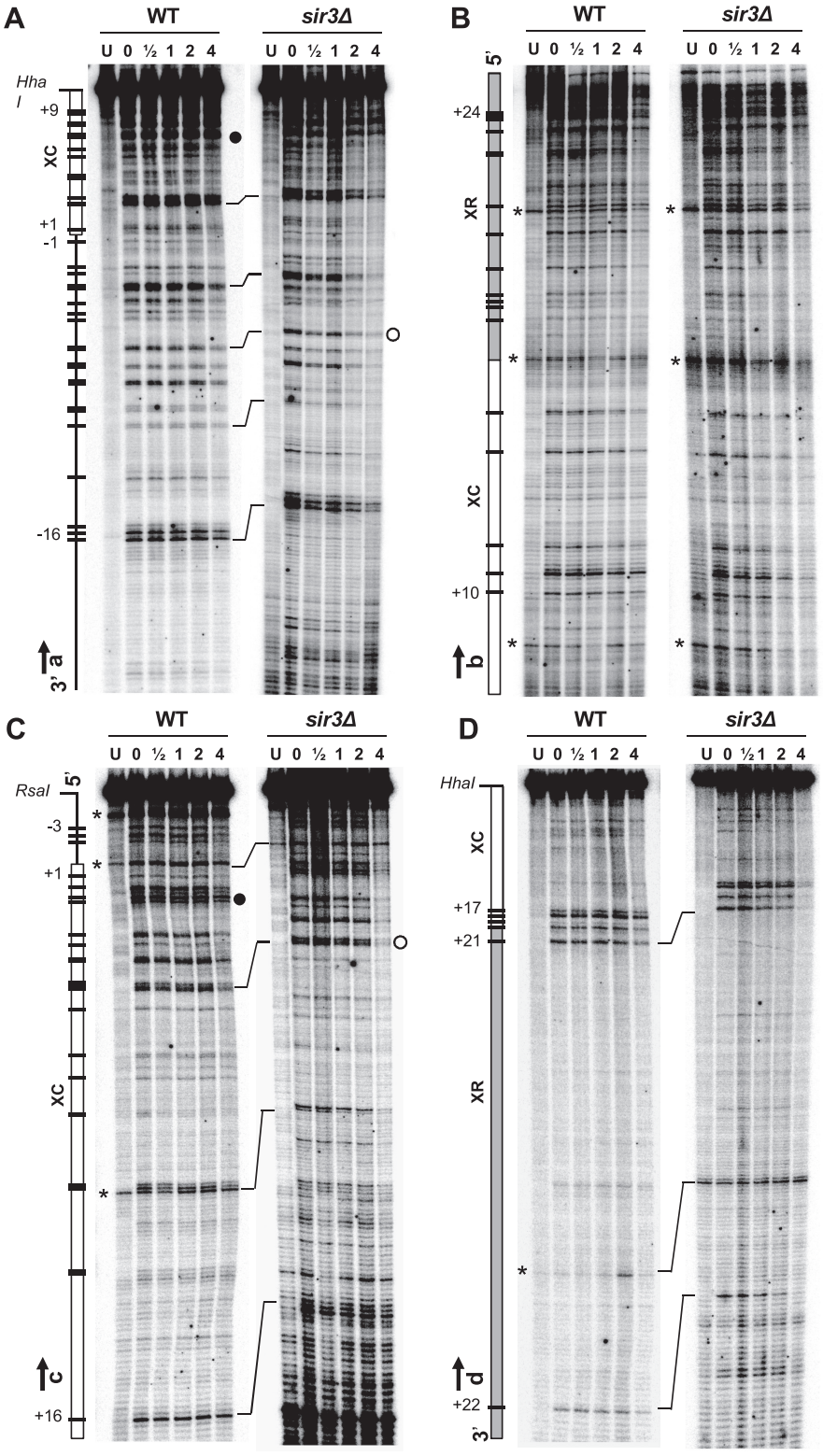

Figure 3. NER in the X element and surrounding region at nucleotide resolution. Yeast were grown and prepared as described in Figure 1, the DNA was extracted and digested with the restriction enzymes HhaI and RsaI (Supplementary Figure S1B), before it was used as template for primer extension. The representative sequencing gels illustrate repair of PDs in the lower (**A** and **B**) and upper (**C** and **D**) strands of WT and *sir3Δ* strains. Lanes are: U, DNA extracted from non-irradiated cells; 0–4, DNA extracted from cells immediately after irradiation or after 0.5, 1, 2 and 4 h repair. Maps on the left sides represent the X element with 3′- and 5′- ends, the XC (white) and XR (gray) regions and the flanking sequences (line). Only PDs that were quantified and plotted in Figure 4 are shown on the maps and are numbered negatively or positively when present outside or inside of the X element, respectively. Stars point to natural sequences causing Taq polymerase arrest; empty and filled circles point to examples of PDs that are fast and slow repaired, respectively; directions for the four primer extensions (a–d) are indicated and brackets align corresponding nucleotides in gels that migrated for different times.

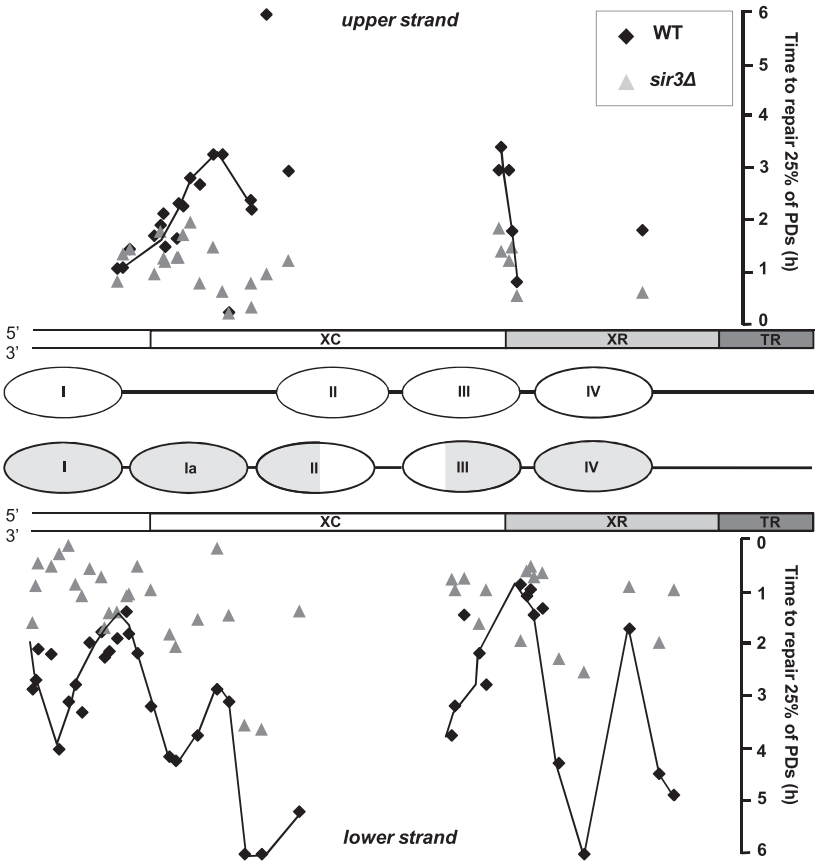

Figure 4. Repair plot of PDs in the X element. Four primers were selected to specifically hybridize with the upper and lower strands in the X element of chromosome 15L (Supplementary Figure S1B, 'a' to 'd'). Quantification of Taq polymerase blocks enabled the calculation of $T_{25\%}$ for each single PD, or for clustered PDs that had similar repair rates. Repair is presented as the time, in hours, needed to remove 25% of PDs at a given site for WT and *sir3Δ* cells. The $T_{25\%}$ values for very slowly repaired PDs ($T_{25\%}$ 5 to 6 h) were calculated by extrapolation of curves where repair of PDs, in percent, was plotted against the repair incubation time (see Supplementary Figure S2A). Black diamonds are for the WT and the lines connecting data points indicate the modulation of NER by nucleosomes; gray triangles are for *sir3Δ*. The map represents the X element with a segment of the flanking 5′ end, the XC- and XR- regions and the telomere repeats (TR). Ovals stand for positioned nucleosomes: upper panel (white), adapted from (23); lower panel (gray), determined by the modulation of NER.

and, generally, it is slow in the center of nucleosome core-DNA and relatively fast in linker DNA between nucleosomes (38,41). Consequently, the resolution of our measurements of repair efficiencies in the X-elements, as shown in Figure 3, should allow observing nucleosome-position dependent modulation of NER. Thus, repair efficiency was quantified and the data plotted as the time needed to remove 25% of PDs against their position in the sequence of the X element, for the upper and lower strand (Figure 4). In WT (black diamonds), the repair rates corroborated the position of nucleosomes mapped by Mavrich *et al*. (nucleosomes I, II, III, IV). In addition, a decrease of the repair rate was observed on both DNA strands on the previously described 330 bp gap, indicating that there could be an additional nucleosome that we labeled 'Ia'. In *sir3Δ* cells (gray triangles) most PDs were removed faster than in the WT and NER efficiency was considerably less modulated, suggesting that Sir3 prevented the movement of nucleosomes that is required for efficient repair (41).

Decreased NER efficiency in Y' elements and chromosome ends is Sir2 and Sir3 independent

There are indications that on the Y' element there are nucleosomes but not Sir proteins (7,23), despite that Y' elements are located between X element and telomeric repeats (Supplementary Figure S1A), both of which have Sir proteins. To analyze NER in Y' sub-telomeres, DNA isolated from WT, *sir2Δ* and *sir3Δ* cells was assayed with the T4-V enzyme, followed by the separation of DNA fragments in denaturing agarose gel electrophoresis and Southern blotting, as described in 'Materials and Methods' section. The membranes were hybridized with a double stranded Y'- probe (Supplementary Figure S1C). There are a short and a long form of Y' element and their copy number is yeast strain dependent, although they are mostly described as one or two copies. For the strain used in this study, restriction enzyme digestion resulted in three DNA fragments with similar lengths (average of ∼4.7 kb), as expected from two adjacent Y' elements (Figure 5A, left panel). Quantitative analyses were obtained by measuring the intensity of the three bands as a single cluster (right panel). For the WT strain, the

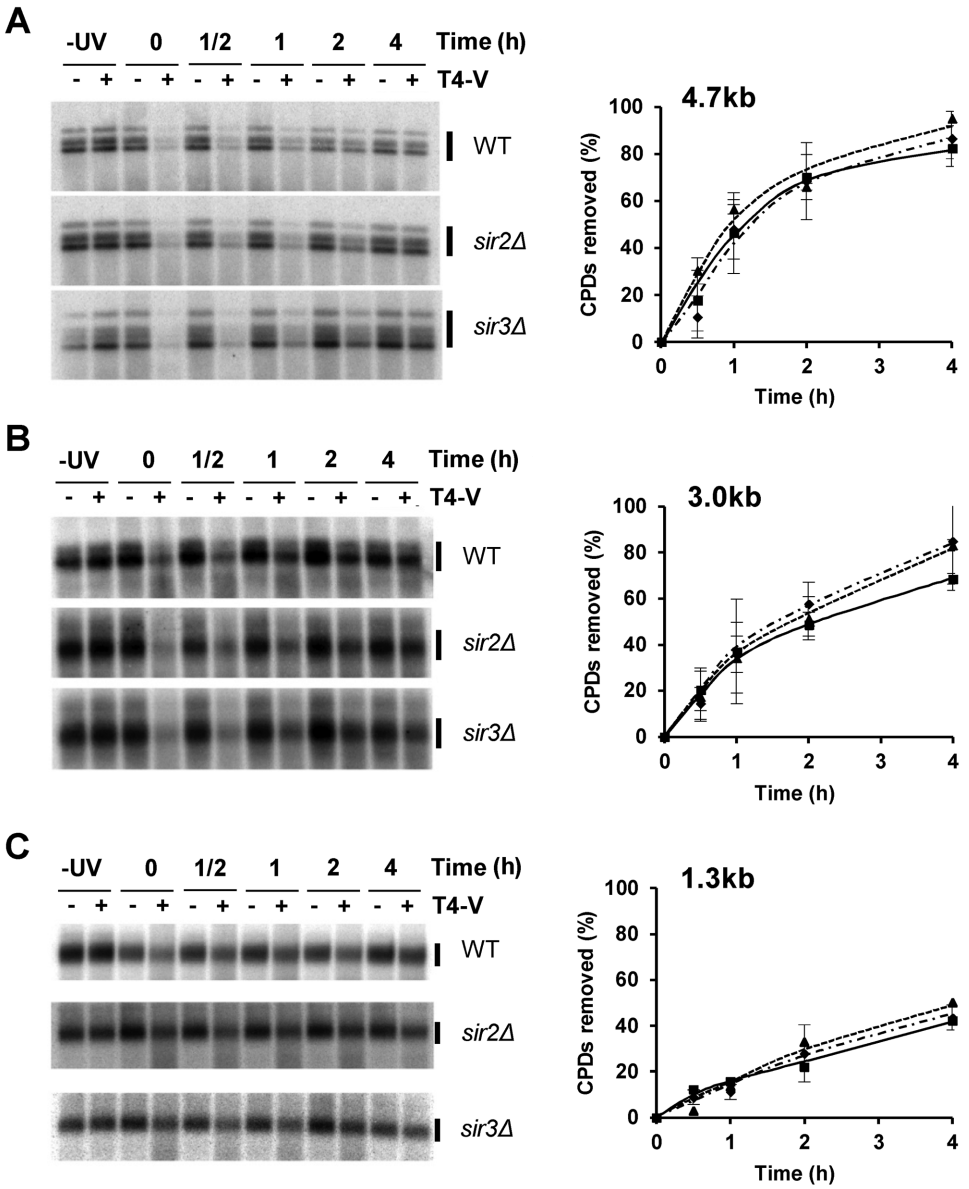

Figure 5. NER within adjacent Y' elements and at chromosome ends. WT, *sir2Δ* and *sir3Δ* cells were irradiated at 180 J/m^2 and harvested at the indicated times (in hours). Isolated DNA from non-irradiated (−UV) and irradiated cells (0–4 h) was digested with EcoRI and HindIII (Supplementary Figure S1C) and mock treated or treated with T4-V, denoted by − and +, respectively. Left panels: after separation of DNA fragments in 1% alkaline agarose-gels and blotting, the membranes were hybridized with the double stranded Y'-probe shown in Supplementary Figure S1C. The resulting band signals represent the average of all Y' elements in the cell. Right panels are the quantification of phosphor images: (**A**) ∼4.7 kb fragment, measurements were taken for the cluster (bracket); (**B**) ∼3.0 kb fragment, made of ∼2.7 kb of the Y' element and ∼0.3 kb of telomeric repeats, measurements were of the broad bands (bracket); (**C**) ∼1.3 kb fragment, made of ∼1 kb Y' element and ∼0.3 kb telomere repeats. Data are for WT (squares), *sir2Δ* (triangles) and *sir3Δ* (diamonds). The means ± 1SD are of three independent experiments.

results indicated that about 46, 70 and 82% of CPDs were removed after 1, 2 and 4 h, respectively. Very similar repair rates were measured in absence of Sir proteins, with percent of CPDs removed of about 56, 66 and 95% (*sir2Δ*), and 48, 68, 86% (*sir3Δ*). These results show that Sir2 and Sir3 proteins present on the neighboring X element and telomeric repeats did not influence NER in the telomere distal region of Y' elements. Thereafter, NER efficiency was followed in the terminal ∼3.0 kb HindIII-fragment that was made of ∼2.65 kb of Y'-sequences and ∼0.35 kb of telomeric repeats, corresponding to ∼88% Y' element and ∼12% telomeric repeat (Supplementary Figure S1C). Within a cell population the length of telomeric repeats varies, resulting in a smeary band, with an average size of ∼3.0 kb (Figure 5B). Quantitative analyses showed that for the WT strain the percent of CPD removed after 1, 2 and 4 h repair were about 37, 49 and 69%. Similar NER efficiencies were found for *sir2Δ* (35, 52 and 83%) and for *sir3Δ* (36, 58 and 85%). Additional information was obtained after digestion with XhoI (Supplementary Figure S1C) that released a population of fragments (broad band) with an average length of ∼1.3 kb (Figure 5C), of which ∼27% was made of telomeric

repeats. Again, the percent of CPDs removed after 1, 2 and 4 h repair was similar for the WT (16, 23 and 43%), the *sir2Δ* (14, 33 and 50%) and the *sir3Δ* (11, 28 and 44%). Thus, in the Y' element NER efficiency was not affected by the presence, or absence, of Sir2 and Sir3 proteins, in agreement with previous observations suggesting that Sir proteins are absent from the Y' element chromatin.

The results presented in Figure 5 show that NER efficiency gradually decreases in a centromere-to-telomere direction (right panels; compare curves for 4.7, 3.0 and 1.3 kb fragments). There are uncharacterized, or dubious, ORFs on both DNA strands of the Y' element (http://www.yeastgenome.org). If they were transcribed, Rad26 dependent TC-NER would remove the UV photoproducts, explaining fast repair of the 4.7 kb fragment. To examine this possibility, NER was followed in *rad26Δ* (TC-NER$^-$) mutants and compared to WT (TC-NER$^+$). The results presented in Supplementary Figure S4 show that there was some Rad26 dependent TC-NER in the Y' elements (compare WT, continuous line with *rad26Δ*, dashed line), corresponding to ∼17% and ∼13% of total repair for the 4.7 and 3.0 kb fragment, respectively, which was calculated as following: repair in WT for each time point was considered as 100%; decreased repair in *rad26Δ* cells was presented as average of the percent for the four repair time points. However, also in *rad26Δ* cells, DNA lesions were removed at different rates from the three DNA fragments and, consequently, putative transcription of short ORFs in the Y' element could not explain the fading of NER efficiency toward the chromosome ends. Thus, we explored whether slow repair of the 1.3 kb terminal fragment was specific for Y'-telomeres. This was assessed by probing telomere VIIL, in a yeast strain where the Y' sub-telomeric region was replaced with the *ADH4* and *URA3* genes, inserted ∼230 bp from the telomeric repeat (Tel07L-modified) (61) (Supplementary Figure S5A). Cells grown in glucose were UV irradiated and DNA repair was followed by the T4-V assay in DNA fragments of different lengths; the terminal ∼1.3 kb fragment containing a portion of the *URA3* gene (∼62% of the fragment) and telomeric repeats (∼27% of the fragment). The results showed similar slow repair rates for both natural (Figure 5C; WT) and synthetic telomeres (Supplementary Figure S5B). Moreover, NER rates decreased with decreasing distance from the telomeric repeat (Supplementary Figure S5B), suggesting that NER was affected by the peculiar chromatin structure near the proximity of chromosome ends.

NER is inhibited by yKu–Sir4 interaction

A core feature of telomere capping is to prevent chromosome fusions, homologous recombination and other illegitimate repair events (10), where the yKu complex plays multiple roles. The yKu heterodimer interacts with Sir4 and this interaction is pivotal for the assembly of telomeric heterochromatin (62–64). Moreover, yKu can directly bind telomeric DNA (65) via its canonical DNA binding activity. However, the recruitment of Sir4 to telomeres can be both, yKu dependent or independent (66). Hence, we considered the possibility that yKu hampered NER close to chromosome ends, as shown in Figure 5C. This was tested in a strain lacking Yku70 (*yku70Δ*), where NER was followed in the three telomere-restriction fragments (Figure 6A). For the 1.3 kb fragment, NER in the *yku70Δ* strain was considerably faster (∼80% CPDs repaired after 4 h) than in the WT (∼40% CPDs repaired after 4 h). For the 4.7 kb fragment, NER efficiency was similar in y*ku70Δ* and WT strains, and for the 3.0 kb fragment, only a slightly faster repair occurred in y*ku70Δ*. As additional control, NER was followed in the *HM* and *MAT* loci, where yKu is not required for the assembly of Sir proteins. These experiments showed that repair of CPDs was very similar in all three loci of both, *yku70Δ* and WT strains (Supplementary Figure S6). All together, these results suggested that yKu inhibited NER specifically at chromosome ends. Given that Sir4 did not inhibit NER in the *HM* and *MAT* loci (Figure 1E), repair of CPDs was analyzed in the three telomere-fragments of the *sir4Δ* strain (Figure 6B). Similar to the measurements obtained for the y*ku70Δ* strain, in the absence of Sir4 repair of CPDs was considerably faster only in the terminal 1.3 kb fragment (∼70% repair after 4 h). To investigate whether the yKu–Sir4 interaction was important for the inhibition of NER, repair of CPDs was investigated in a yeast strain carrying a mutated *YKU80* allele. The Yku80-L140A protein by and large has lost its ability to interact with Sir4 but yKu binds normally to DNA. Yeast carrying the *yku80-L140* allele displays deficient TPE but telomere integrity is not affected (65,67). The results obtained with the T4-V assay (Figure 6C) show that CPDs are fast removed in the terminal 1.3 kb fragment (∼75% repair after 4 h), suggesting that yKu–Sir4 binding inhibits NER.

In addition to the multiple functions of yKu described above, yKu is needed for repair by non-homologous end joining (NHEJ), but not for homologous recombination (68,69). One model proposes that yKu in conjunction with Sir proteins forms a chromatin structure that is essential for rejoining broken DNA ends (62). To determine if NHEJ participated in repair of UV damaged sub-telomeric Y' elements, the presence of CPDs was followed in *nej1Δ* (NHEJ$^-$/NER$^+$) (70,71) and compared to WT (NHEJ$^+$/NER$^+$). The results shown in Supplementary Figure S7 imply that NHEJ does not contribute to repair of CPDs in the three fragments of chromosome ends.

DISCUSSION

In this study, repression of NER by heterochromatin was assessed at *HM* loci and natural telomeres. Previously, NER was investigated at chromosome ends lacking sub-telomeric sequences, which were replaced with the *URA3* gene (synthetic telomeres). It was found that the efficiency of NER in *URA3* was modulated by alterations in chromatin structure associated with silencing, because repression of NER was released in *sir3Δ* and *sir2Δ* cells (43,44). The two reports were based on evidence for TPE-associated repression of genes and on a model of large domains of repressive chromatin that is formed by a continuous gradient of Sir proteins, spreading from the most distal telomere terminal repeats. However, recent reports indicate that Sir proteins are not continuously distributed at natural telomeres. The ChIP-seq assay identified the Sir complex on the X elements and on telomeric repeats but not on the Y' elements. Conse-

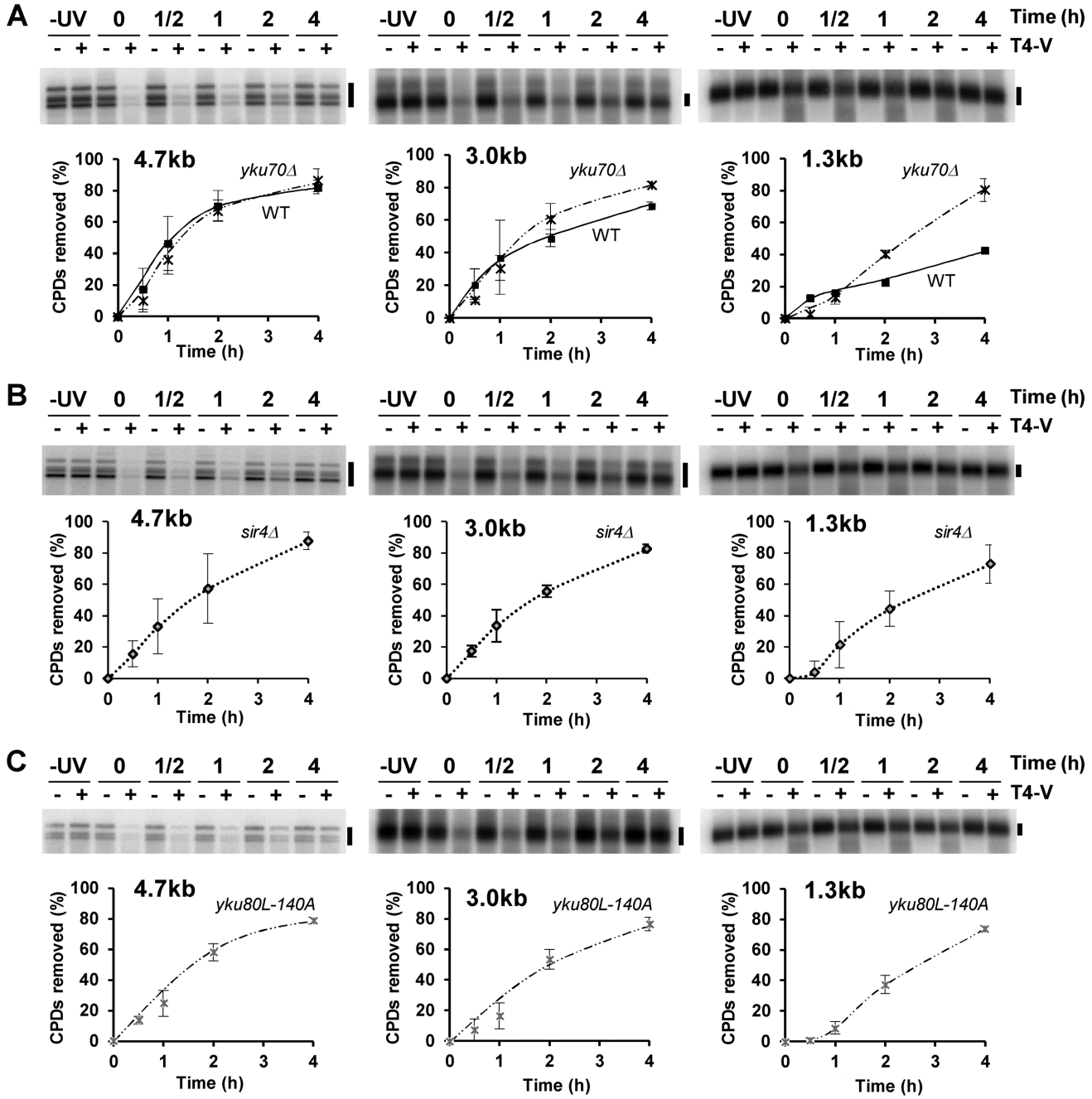

Figure 6. NER in y*kuΔ*, *sir4Δ* and *yku80L-140A* cells. DNA preparations were done as described in the legend of Figure 5. Upper panels are representative T4-V assays, lower panels are quantifications of phosphor images. (**A**) *kuΔ* (*yku70Δ*): WT, squares and continuous line; y*kuΔ*, crosses and dashed line. Curves for the WT are as in Figure 5 and were used here for comparison. (**B**) *sir4Δ* and (**C**) *yku80L-140A*. The means ± 1SD are of three independent experiments.

quently, models for transcription and NER repression mediated by natural telomeric chromatin need further investigation.

Yeast heterochromatin is formed by the recruitment of silencing complexes to nucleosomes with definite modified histones (72). Although there is considerable knowledge on Sir proteins, their spreading and interactions with histones, the extent to which Sir proteins affect nucleosome stability and DNA accessibility is little understood. It is proposed that silencing occurs by occlusion of transcription factors from the cognate DNA element, for example by stabilizing a nucleosome on gene promoters (43,73). Since heterochromatin of natural X sub-telomeric regions is built by the interactions of Sir proteins with oligo-nucleosomes (20,60), we considered the whole X element as archetype substrate to investigate NER accessibility to UV-induced DNA lesions in heterochromatin. Specific oligo DNA-primers were designed to follow damage formation and NER in the X el-

ement of chromosome XV-L. The results showed that repair of photoproducts was considerably slow over the entire X element. In absence of Sir3 NER efficiency increased significantly, reaching rates that were somewhat faster than those measured in array of positioned nucleosomes in the non-transcribed regions of the rDNA locus, but slower than those measured in the highly transcribed rRNA genes (Supplementary Figure S8). Additional information was obtained by measuring the repair rates for individual DNA lesion in the X element. It is well established that photoproducts are repaired fast in linker DNA and toward the end of positioned nucleosomes, but slow in the center of nucleosomal core DNA. Cyclic modulation of NER was first observed in the yeast *URA3* gene (39) and related to the position of nucleosomes described by a different study (74). Thereafter, a number of investigations confirmed that positioned nucleosomes modulated repair efficiency (41). Thus, it became evident that repair-analysis of photoproducts at nucleotide precision was a valuable tool to determine the position of nucleosomes *in vivo* (75). Since the occurrence of histones on X elements has been controversial (20,23), we exploited the distinctive modulation of NER to assess nucleosomes in the X element. The efficiency of repair followed a periodicity of ∼130 bp that is characteristic for NER in nucleosomal DNA. Remarkably, in the absence of Sir3 excision of photoproducts was faster and largely not modulated, as described for chromatin regions with unstable nucleosomes (38,41). Hence, we propose that the Sir complex stabilizes the position of nucleosomes on the X element. Because PDs can be exposed to NER factors during transient shifts in nucleosome positioning (38,41), we suggest that the slow NER in the X element heterochromatin results from the reduced mobility of nucleosomes.

In comparison, NER was followed in Y' chromatin that is characterized by arrays of nucleosomes but lack Sir proteins (7,20). It was not possible to design primers that annealed with only the short or the long forms of Y' elements, without unspecific cross-hybridization. Therefore, NER activity was measured by the T4-V assay in three subsequent segments of the Y' sequence, and the results represented the average of DNA damage and repair that occurred in all Y' telomeres. Parallel experiments in the mating type locus validated that the T4-V assay could discriminate between NER efficiencies in Sir containing versus Sir depleted chromatin. In the sub-telomeric Y' loci of WT, *sir2Δ* and *sir3Δ* strains CPDs were repaired at similar rates. These results corroborate genome-wide ChIP data for the localization of Sir proteins, which indicated that they were not present on Y' elements (7). Moreover, the most distant fragment from the telomeric repeat, formed only by Y' sequences, was repaired very fast, like the transcribed *MATa* gene. Some of the fast repair resulted from TC-NER, because removal of DNA lesions was less efficient in the *rad26Δ* strain. At the extreme end of chromosomes, NER was analyzed in a fragment of ∼1.3 kb (TRF) composed by ∼ 25% of terminal telomeric repeats buried in a specialized structure that includes Sir 2, 3, 4 and yKu proteins, but lacks histones (20,22,72). A model for spreading of heterochromatin at telomeres proposes that Yku80 interacts with Sir4 that is bound at telomeres, and that this interaction promotes the recruitment of Sir3 (63). However, yKu can also bind directly to telomeric DNA (65). Surprisingly, NER efficiency in the TRF did not increase in cells lacking Sir2 or Sir3. Conversely, it increased considerably in the absence of Yku or Sir4, pointing out that the yKu–Sir4 interaction inhibits NER. This was confirmed when repair of CPDs was investigated in a yeast strain carrying a mutated *YKU80* allele. Despite both yKu and Sir4 being present, their interaction is reduced in *yku80-L140A* cells (67) and CPDs are fast removed from the TRF. Further investigations will be required to explain how the yKu–Sir4 interaction inhibits NER. In fact, the Ku complex binds non-specifically to DNA breaks to promote repair by NHEJ (62), but we confirmed that NHEJ did not contribute to repair of CPDs near the proximity of chromosome ends. Therefore, our data are more consistent with the possibility that the inhibition of NER near telomeric repeats is associated with an alternative function of yKu, which occurs at non-terminal sites (65).

In summary, studies on NER at natural telomeres have been limited to mammalian cells and the results remains contradictory. An early study on genomic heterogeneity of DNA repair showed that human somatic cells efficiently removed PDs from telomeric DNA (76). This conclusion was recently supported by findings obtained with human fibroblasts expressing exogenous telomerase, showing that CPDs in telomeres were repaired at a faster rate than CPDs in the bulk of the genome (77). In contrast, Rochette *et al.* (78) found that CPDs are not repaired in telomeres, that cells tolerate persistent high levels of damaged telomeric DNA and that they continue proliferating without showing changes in telomere lengths. Our results are more consistent with the latter findings, but more investigations that consider the structure of chromatin are needed to help determining the activity of NER at natural telomeres.

SUPPLEMENTARY DATA

Supplementary Data are available at NAR Online.

ACKNOWLEDGEMENTS

We thank Dr. Patrick Rochette (University Laval, Québec) for critical reading of the manuscript and the reviewers for insightful discussion.
Author contributions: L.G. and A.D'A. were equally supported by A.C. and R.J.W.; both M.T.s were supported by A.C. Consumables were provided by A.C. and publication fees by R.J.W. L.G, A.C. and R.J.W. designed the research and wrote the manuscript; L.G., both M.T.s and A.D'A. performed the T4-V assays, L.G. and R.E.W. performed the primer extensions.

FUNDING

Natural Sciences and Engineering Research Council of Canada (NSERC) (to A.C.); Canadian Institutes of Health Research (CIHR) [97874 to R.J.W.]; Spanish Ministry of Science and Innovation (MINECO) [BFU2015-69183-P to R.E.W.] and European Union (FEDER) (to R.E.W.). Funding for open access charge: CIHR [97874 to R.J.W.].
Conflict of interest statement. None declared.

REFERENCES

1. Sherstyuk,V.V., Shevchenko,A.I. and Zakian,S.M. (2014) Epigenetic landscape for initiation of DNA replication. *Chromosoma*, **123**, 183–199.
2. Annunziato,A.T. (2015) The fork in the road: histone partitioning during DNA replication. *Genes*, **6**, 353–371.
3. Conconi,A. (2015) Preface. *DNA Repair (Amst)*, **36**, 5–6.
4. Lawrence,M., Daujat,S. and Schneider,R. (2016) Lateral thinking: how histone modifications regulate gene expression. *Trends Genet.*, **32**, 42–56.
5. Hoppe,G.J., Tanny,J.C., Rudner,A.D., Gerber,S.A., Danaie,S., Gygi,S.P. and Moazed,D. (2002) Steps in assembly of silent chromatin in yeast: Sir3-independent binding of a Sir2/Sir4 complex to silencers and role for Sir2-dependent deacetylation. *Mol. Cell Biol.*, **22**, 4167–4180.
6. Rusche,L.N., Kirchmaier,A.L. and Rine,J. (2003) The establishment, inheritance, and function of silenced chromatin in Saccharomyces cerevisiae. *Annu. Rev. Biochem.*, **72**, 481–516.
7. Thurtle,D.M. and Rine,J. (2014) The molecular topography of silenced chromatin in Saccharomyces cerevisiae. *Genes Dev.*, **28**, 245–258.
8. Weiss,K. and Simpson,R.T. (1998) High-resolution structural analysis of chromatin at specific loci: Saccharomyces cerevisiae silent mating type locus HMLalpha. *Mol. Cell. Biol.*, **18**, 5392–5403.
9. Ravindra,A., Weiss,K. and Simpson,R.T. (1999) High-resolution structural analysis of chromatin at specific loci: Saccharomyces cerevisiae silent mating-type locus HMRa. *Mol. Cell. Biol.*, **19**, 7944–7950.
10. Wellinger,R.J. and Zakian,V.A. (2012) Everything you ever wanted to know about Saccharomyces cerevisiae telomeres: beginning to end. *Genetics*, **191**, 1073–1105.
11. Gottschling,D.E., Aparicio,O.M., Billington,B.L. and Zakian,V.A. (1990) Position effect at S. cerevisiae telomeres: reversible repression of Pol II transcription. *Cell*, **63**, 751–762.
12. Sandell,L.L. and Zakian,V.A. (1992) Telomeric position effect in yeast. *Trends Cell Biol.*, **2**, 10–14.
13. Aparicio,O.M., Billington,B.L. and Gottschling,D.E. (1991) Modifiers of position effect are shared between telomeric and silent mating-type loci in S. cerevisiae. *Cell*, **66**, 1279–1287.
14. Strahl-Boslinger,S., Hecht,A., Luo,K. and Grunstein,M. (1997) SIR2 and SIR4 interactions differ in core and extended telomeric heterochromatin in yeast. *Genes Dev.*, **11**, 83–93.
15. Boulton,S.J. and Jackson,S.P. (1998) Components of the Ku-dependent non-homologous end-joining pathway are involved in telomeric length maintenance and telomeric silencing. *EMBO J.*, **17**, 1819–1828.
16. Laroche,T., Martin,S.G., Gotta,M., Gorham,H.C., Pryde,F.E., Louis,E.J. and Gasser,S.M. (1998) Mutation of yeast Ku genes disrupts the subnuclear organization of telomeres. *Curr. Biol.*, **8**, 653–656.
17. Zill,O.A., Scannell,D., Teytelman,L. and Rine,J. (2010) Co-evolution of transcriptional silencing proteins and the DNA elements specifying their assembly. *PLoS Biol.*, **8**, e1000550.
18. Radman-Livaja,M., Ruben,G., Weiner,A., Friedman,N., Kamakaka,R. and Rando,O.J. (2011) Dynamics of Sir3 spreading in budding yeast: secondary recruitment sites and euchromatic localization. *EMBO J.*, **30**, 1012–1026.
19. Li,M., Valsakumar,V., Poorey,K., Bekiranov,S. and Smith,J.S. (2013) Genome-wide analysis of functional sirtuin chromatin targets in yeast. *Genome Biol.*, **14**, R48.
20. Zhu,X. and Gustafsson,C.M. (2009) Distinct differences in chromatin structure at subtelomeric X and Y' elements in budding yeast. *PLOS One*, **4**, e6363.
21. Pryde,F.E. and Louis,E.J. (1999) Limitations of silencing at native telomeres. *EMBO J.*, **18**, 2538–2550.
22. Wright,J.H., Gottschling,D.E. and Zakian,V.A. (1992) Saccharomyces telomeres assume a non-nucleosomal chromatin structure. *Genes Dev.*, **6**, 197–210.
23. Mavrich,T.N., Ioshikhes,I.P., Venters,B.J., Jiang,C., Tomsho,L.P., Qi,J., Schuster,S.C., Albert,I. and Pugh,B.F. (2008) A barrier nucleosome model for statistical positioning of nucleosomes throughout the yeast genome. *Genome Res.*, **18**, 1073–1083.
24. Maillet,L., Boscheron,C., Gotta,M., Marcand,S., Gilson,E. and Gasser,S.M. (1996) Evidence for silencing compartments within the yeast nucleus: a role for telomere proximity and Sir protein concentration in silencer-mediated repression. *Genes Dev.*, **10**, 1796–1811.
25. Laroche,T., Martin,S.G., Tsai-Pflugfelder,M. and Gasser,S.M. (2000) The dynamics of yeast telomeres and silencing proteins through the cell cycle. *J. Struct. Biol.*, **129**, 159–174.
26. Tham,W.H., Wyithe,J.S., Ko Ferrigno,P., Silver,P.A. and Zakian,V.A. (2001) Localization of yeast telomeres to the nuclear periphery is separable from transcriptional repression and telomere stability functions. *Mol. Cell*, **8**, 189–199.
27. Gravel,S., Larrivee,M., Labrecque,P. and Wellinger,R.J. (1998) Yeast Ku as a regulator of chromosomal DNA end structure. *Science*, **280**, 741–744
28. Taddei,A., Hediger,F., Neumann,F.R., Bauer,C. and Gasser,S.M. (2004) Separation of silencing from perinuclear anchoring functions in yeast Ku80, Sir4 and Esc1 proteins. *EMBO J.*, **23**, 1301–1312.
29. Taddei,A., Schober,H. and Gasser,S.M. (2010) The budding yeast nucleus. *Cold Spring Harb.*, **2**, a000612.
30. Spivak,G. (2015) Nucleotide excision repair in humans. *DNA Repair (Amst)*, **36**, 13–18.
31. Mullenders,L. (2015) DNA damage mediated transcription arrest: step back to go forward. *DNA Repair (Amst)*, **36**, 28–35.
32. Verhage,R., Zeeman,A.M., de Groot,N., Gleig,F., Bang,D.D., van de Putte,P. and Brouwer,J. (1994) The RAD7 and RAD16 genes, which are essential for pyrimidine dimer removal from the silent mating type loci, are also required for repair of the nontranscribed strand of an active gene in Saccharomyces cerevisiae. *Mol. Cell. Biol.*, **14**, 6135–6142.
33. Prakash,S. and Prakash,L. (2000) Nucleotide excision repair in yeast. *Mutat. Res.*, **451**, 13–24.
34. van Gool,A.J., Verhage,R., Swagemakers,S.M.A., van de Putte,P., Brouwer,J., Troelstra,C., Bootsma,D. and Hoeijmakers,J.H.J. (1994) RAD26, the functional S. cerevisiae homolog of the Cockayne syndrome B gene ERCC6. *EMBO J.*, **13**, 5361–5369.
35. Tremblay,M., Teng,Y., Paquette,M., Waters,R. and Conconi,A. (2008) Complementary roles of yeast Rad4p and Rad34p in nucleotide excision repair of active and inactive rRNA gene chromatin. *Mol. Cell. Biol.*, **28**, 7504–7513.
36. Mellon,I., Spivak,G. and Hanawalt,P.C. (1987) Selective removal of transcription-blocking DNA damage from the transcribed strand of the mammalian DHFR gene. *Cell*, **51**, 241–249.
37. Hanawalt,P.C. and Spivak,G. (2008) Transcription-coupled DNA repair: two decades of progress and surprises. *Nat. Rev.*, **9**, 958–970.
38. Wellinger,R.E. and Thoma,F. (1997) Nucleosome structure and positioning modulate nucleotide excision repair in the non-transcribed strand of an active gene. *EMBO J.*, **16**, 5046–5056.
39. Tijsterman,M., de Pril,R., Tasseron-de Jong,J.G. and Brouwer,J. (1999) RNA polymerase II transcription suppresses nucleosomal modulation of UV-induced (6-4) photoproduct and cyclobutane pyrimidine dimer repair in yeast. *Mol. Cell. Biol.*, **19**, 934–940.
40. Powell,N.G., Ferreiro,J., Karabetsou,N., Mellor,J. and Waters,R. (2003) Transcription, nucleosome positioning and protein binding modulate nucleotide excision repair of the Saccharomyces cerevisiae MET17 promoter. *DNA Repair*, **2**, 375–386.
41. Guintini,L., Charton,R., Peyresaubes,F., Thoma,F. and Conconi,A. (2015) Nucleosome positioning, nucleotide excision repair and photoreactivation in Saccharomyces cerevisiae. *DNA Repair (Amst)*, **36**, 98–104.
42. Jia,P., Her,C. and Chai,W. (2015) DNA excision repair at telomeres. *DNA Repair (Amst)*, **36**, 137–145.
43. Livingstone-Zatchej,M., Marcionelli,R., Moller,K., de Pril,R. and Thoma,F. (2003) Repair of UV lesions in silenced chromatin provides in vivo evidence for a compact chromatin structure. *J. Biol. Chem.*, **278**, 37471–37479.
44. Irizar,A., Yu,Y., Reed,S.H., Louis,E.J. and Waters,R. (2010) Silenced yeast chromatin is maintained by Sir2 in preference to permitting histone acetylations for efficient NER. *Nucleic Acids Res.*, **38**, 4675–4686.
45. Winzeler,E.A., Shoemaker,D.D., Astromoff,A., Liang,H., Anderson,K., Andre,B., Bangham,R., Benito,R., kmBoeke,J.D., Bussey,H. *et al.* (1999) Functional characterization of the S. cerevisiae genome by gene deletion and parallel analysis. *Science*, **285**, 901–906.

46. Conconi,A. (2008) Yeast as model system to study DNA damage and DNA repair. In: Conn,PM (ed). *Sourcebook of Models for Biomedical Research*. Humana Press Inc., Totowa, pp. 445–453.
47. Conconi,A., Widmer,R.M., Koller,T. and Sogo,J.M. (1989) Two different chromatin structures coexist in ribosomal RNA genes throughout the cell cycle. *Cell*, **57**, 753–761.
48. Pelloux,J., Tremblay,M., Wellinger,R.J. and Conconi,A. (2012) UV-induced DNA damage and DNA repair in ribosomal genes chromatin. In: Vancura,A (ed). *Transcriptional Regulation: Methods and Protocols, Methods in Molecular Biology*. Humana Press, NY, Vol. **809**, pp. 303–320.
49. Bespalov,V.A., Conconi,A., Zhang,X., Fahy,D. and Smerdon,M.J. (2001) Improved method for measuring the ensemble average of strand breaks in genomic DNA. *Environ. Mol. Mutagen.*, **38**, 166–174.
50. Loo,S. and Rine,J. (1994) Silencers and domains of generalized repression. *Science*, **264**, 1768–1771.
51. Chen,L. and Widom,J. (2005) Mechanism of transcription silencing in yeast. *Cell*, **120**, 37–48.
52. Gao,L. and Gross,D.S. (2008) Sir2 silences gene transcription by targeting the transition between RNA polymerase II initiation and elongation. *Mol. Cell. Biol.*, **28**, 3979–3994.
53. Holland,M.J. (2002) Transcript abundance in yeast varies over six orders of magnitude. *J. Biol. Chem.*, **277**, 14363–14366.
54. Wang,X., Bryant,G., Zhao,A. and Ptashne,M. (2015) Nucleosome avidities and transcriptional silencing in yeast. *Curr. Biol.*, **25**, 1215–1220.
55. Terleth,C., Schenk,P., Poot,R., Brouwer,J. and van de Putte,P. (1990) Differential repair of UV damage in rad mutants of Saccharomyces cerevisiae: a possible function of G2 arrest upon UV irradiation. *Mol. Cell. Biol.*, **10**, 4678–4684
56. Chaudhuri,S., Wyrick,J.J. and Smerdon,M.J. (2009) Histone H3 Lys79 methylation is required for efficient nucleotide excision repair in a silenced locus of Saccharomyces cerevisiae. *Nucleic Acids Res.*, **37**, 1690–1700.
57. Wellinger,R.E. and Thoma,F. (1996) Taq DNA polymerase blockage at pyrimidine dimers. *Nucleic Acids Res.*, **24**, 1578–1579.
58. Conconi,A., Liu,X., Koriazova,L., Ackerman,E.J. and Smerdon,M.J. (1999) Tight correlation between inhibition of dna repair in vitro and transcription factor IIIA binding in the 5S ribosomal gene. *EMBO J.*, **18**, 1387–1396.
59. Smerdon,M.J. and Conconi,A. (1999) Modulation of DNA damage and DNA repair in chromatin. In: Moldave,K (ed). *Progress in Nucleic Acids Research and Molecular Biology*, Academic Press, Inc., Vol. **62**, pp. 227–255.
60. de Bruin,D., Kantrow,S.M., Liberatore,R.A. and Zakian,V.A. (2000) Telomere folding is required for the stable maintenance of telomere position effects in yeast. *Mol. Cell. Biol.*, **20**, 7991–8000.
61. Maicher,A., Kastner,L., Dees,M. and Luke,B. (2012) Deregulated telomere transcription causes replication-dependent telomere shortening and promotes cellular senescence. *Nucleic Acids Res.*, **40**, 6649–6659.
62. Tsukamoto,Y., Kato,J. and Ikeda,H. (1997) Silencing factors participate in DNA repair and recombination in Saccharomyces cerevisiae. *Nature*, **388**, 900–903.
63. Roy,R., Meier,B., McAinsh,A.D., Feldmann,H.M. and Jackson,S.P. (2004) Separation-of-function mutants of yeast Ku80 reveal a Yku80p-Sir4p interaction involved in telomeric silencing. *J. Biol. Chem.*, **279**, 86–94.
64. Hass,E.P. and Zappulla,D.C. (2015) The Ku subunit of telomerase binds Sir4 to recruit telomerase to lengthen telomeres in S. cerevisiae. *Elife*, **4**, e07750.
65. Larcher,M.V., Pasquier,E., MacDonald,R.S. and Wellinger,R.J. (2016) Ku binding on telomeres occurs at sites distal from the physical chromosome ends. *PLoS Genet.*, **12**, e1006479.
66. Luo,K., Vega-Palas,M.A. and Grunstein,M. (2002) Rap1-Sir4 binding independent of other Sir, yKu, or histone interactions initiates the assembly of telomeric heterochromatin in yeast. *Genes Dev.*, **12**, 1528–1539.
67. Ribes-Zamora,A., Mihalek,I., Lichtarge,O. and Bertuch,A.A. (2007) Distinct faces of the Ku heterodimer mediate DNA repair and telomeric functions. *Nat. Stru. Mol. Biol.*, **14**, 301–307.
68. Milne,G.T., Jin,S., Shannon,K.B. and Weaver,D.T. (1996) Mutations in two Ku homologs define a DNA end-joining repair pathway in Saccharomyces cerevisiae. *Mol. Cell. Biol.*, **8**, 4189–4198.
69. Boulton,S.J. and Jackson,S.P. (1996) Saccharomyces cerevisiae Ku70 potentiates illegitimate DNA double-strand break repair and serves as a barrier to error-prone DNA repair pathways. *EMBO J.*, **18**, 5093–5103.
70. Valencia,M., Bentele,M., Vaze,M.B., Herrmann,G., Kraus,E., Lee,S.E., Schär,P. and Haber,J.E. (2001) NEJ1 controls non-homologous end joining in Saccharomyces cerevisiae. *Nature*, **6864**, 666–669.
71. Kegel,A., Sjöstrand,J.O. and Aström,S.U. (2001) Nej1p, a cell type-specific regulator of nonhomologous end joining in yeast. *Curr. Biol.*, **20**, 1611–1617.
72. Oppikofer,M., Kueng,S. and Gasser,S.M. (2013) SIR-nucleosome interactions: structure-function relationships in yeast silent chromatin. *Gene*, **527**, 10–25.
73. Aparicio,O.M. and Gottschling,D.E. (1994) Overcoming telomeric silencing: a trans-activator competes to establish gene expression in a cell cycle-dependent way. *Genes Dev.*, **8**, 1133–1146.
74. Tanaka,S.M., Livingstone-Zatchej,M. and Thoma,F. (1996) Chromatin structure of the yeast URA3 gene at high resolution provides insight into structure and positioning of nucleosomes in the chromosomal context. *J. Mol. Biol.*, **257**, 919–934.
75. Tremblay,M., Toussaint,M., D'Amours,A. and Conconi,A. (2009) Nucleotide excision repair and photolyase repair of UV photoproducts in nucleosomes; assessing the existence of nucleosome and non-nucleosome rDNA chromatin in vivo. *Biochem. Cell Biol.*, **87**, 337–346.
76. Kruk,P.A., Rampino,N.J. and Bohr,V.A. (1995) DNA damage and repair in telomeres: relation to aging. *Proc. Natl. Acad. Sci. U.S.A.*, **92**, 258–262.
77. Parikh,D., Fouquerel,E., Murphy,C.T., Wang,H. and Opresko,P.L. (2015) Telomeres are partly shielded from ultraviolet-induced damage and proficient for nucleotide excision repair of photoproducts. *Nat. Commun.*, **6**, 8214.
78. Rochette,P.J. and Brash,D.E. (2010) Human telomeres are hypersensitive to UV-induced DNA damage and refractory to repair. *PLoS Genet.*, **6**, e1000926.